Dalton Transactions

PAPER

View Article Online
View Journal | View Issue

Open Access Article. Published on 20 April 2015. Downloaded on 11/26/2024 12:58:05 AM.
This article is licensed under a Creative Commons Attribution 3.0 Unported Licence.

Cite this: *Dalton Trans.*, 2015, **44**, 9569

Hydrothermal synthesis of Group 13 metal trifluoride complexes with neutral N-donor ligands†‡

Rajiv Bhalla,[a] William Levason,[b] Sajinder K. Luthra,[c] Graeme McRobbie,[c] Francesco M. Monzittu,[b] Jazmyn Palmer,[b] Gillian Reid,*[b] George Sanderson[b] and Wenjian Zhang[b]

Received 20th March 2015,
Accepted 20th April 2015

DOI: 10.1039/c5dt01120e

www.rsc.org/dalton

The reactions of the hydrated Group 13 fluorides, $MF_3{\cdot}3H_2O$ (M = Al, Ga or In) with 2,2′:6′,2″-terpyridyl, 2,2′-bipyridyl or 1,10-phenanthroline under hydrothermal conditions (180 °C/15 h) produced high yields of the complexes $[MF_3(terpy)]{\cdot}3H_2O$, $[MF_3(bipy)(OH_2)]{\cdot}2H_2O$ and $[MF_3(phen)(OH_2)]$. X-Ray crystal structures of $[M'F_3(terpy)]{\cdot}3H_2O$ (M′ = Al or Ga), $[M'F_3(bipy)(OH_2)]{\cdot}2H_2O$ and $[GaF_3(phen)(OH_2)]$ show that all of them contain distorted octahedral geometries at the metal with *mer*-trifluoride coordination. Extensive H-bonding (F···H–OH) links the molecules. The complexes have been further characterised by microanalysis, IR, ^{1}H, ^{19}F{^{1}H} and ^{27}Al NMR spectroscopy. In contrast, reactions of the trifluorides with the acyclic triamine, *N*,*N*,*N*′,*N*′,*N*″-pentamethyldiethylenetriamine, under similar hydrothermal conditions results in cleavage of the triamine and ring-closure to form the 1,1,4-trimethylpiperazinium cation, $[\subset Me_2N(CH_2)_2NMe(CH_2)_2]^+$, with fluorometallate anions, and confirmed by X-ray analysis of $[\subset Me_2N(CH_2)_2NMe(CH_2)_2]_2[Al_2F_8(OH_2)_2]{\cdot}2H_2O$. The strongly H-bonded $[GaF_3(terpy)]{\cdot}3H_2O$ was also obtained by Cl/F exchange from $[GaCl_3(terpy)]$ and $[NBu_4]F$ or [K(2,2,2-crypt)]F. Crystallisation of a mixture of $[NH_4][PF_6]$ and $[GaF_3(terpy)]{\cdot}3H_2O$ from aqueous solution produced the edge-bridged cationic complex, $[\{Ga(terpy)F\}_2(\mu\text{-}F)_2][PF_6]_2$. The synthesis of the more sterically bulky $[GaCl_3(^tBu_3\text{-terpy})]$ ($^tBu_3$-terpy = 4,4′4″-tris-^{t}Bu-2,2′:6′,2″-terpyridyl) and the crystal structure of $[GaCl_2(^tBu_3\text{-terpy})][GaCl_4]$, which contains a trigonal bipyramidal cation, are also reported.

Introduction

The anhydrous Group 13 metal fluorides MF_3 (M = Al, Ga or In) are inert polymeric solids and generally unreactive towards neutral ligands. This has hindered attempts to explore their coordination chemistry, hence very few adducts have been described.[1] The hydrates, $MF_3{\cdot}3H_2O$, are more reactive, but have very poor solubility in organic solvents or water.[1] Two structural forms of $AlF_3{\cdot}3H_2O$ are known, the α-form with discrete $[AlF_3(OH_2)_3]$ molecules, and the β-form which is a polymer, $[\{AlF_2(OH_2)_2(\mu\text{-}F)\}_n]{\cdot}nH_2O$.[2] The structure of $GaF_3{\cdot}3H_2O$ is unclear, but $InF_3{\cdot}3H_2O$ is also a fluoride bridged polymer.[2] Prolonged reflux of $GaF_3{\cdot}3H_2O$ with pyridine in thf afforded the *mer* octahedral complex $[GaF_3(py)_3]$,[3] whilst the reaction of $GaF_3{\cdot}3H_2O$ with 1,4,7-tris(2-amino-3,5-di-*tert*-butylbenzyl)-1,4,7-triazacyclononane (L) under reflux conditions in ethanol, followed by crystallisation from MeOH, afforded $[GaF_3(L)]{\cdot}6MeOH$, as an S_6-symmetric MeOH hexamer.[4] Complexes of aluminium, gallium and indium fluorides with (neutral) NH_3 ligands have been formed from the reaction of AlN or InN with NH_4F in supercritical ammonia at 400 °C, from NH_4F or NH_4HF_2 and elemental Ga, and from $[NH_4]_3[MF_6]$ and gaseous NH_3, or $MF_3{\cdot}3H_2O$ and liquid NH_3.[5–9] The structures are usually polymeric with F-bridges. Studies in aqueous solution of various ethylenediamine derivatives of Al and Ga[10,11] and of the indium fluoride-2,2′-bipyridyl-H_2O-HF system[12] have also been reported. The X-ray crystal structures of $[InF_3(2,2'\text{-bipy})(OH_2)]{\cdot}2H_2O$ and $[InF_3(phen)(OH_2)]$ obtained during the latter study have been described.[12,13] The complexes $[MF_3(4,4'\text{-bipy})]$ (M = Ga and In) were formed hydrothermally from the respective $MF_3{\cdot}3H_2O$ and 4,4′-bipyridyl in aqueous HF at 180 °C.[14] Hydrothermal synthesis has also been used with other N-donor ligands such as the macrocyclic Me_3-tacn and $BzMe_2$-tacn (Me_3-tacn = 1,4,7-trimethyl-1,4,7-triazacyclononane, $BzMe_2$-tacn = 1,4,dimethyl-7-benzyl-1,4,7-triaza-

[a]*Centre for Advanced Imaging, University of Queensland, Brisbane, Queensland 4072, Australia*
[b]*School of Chemistry, University of Southampton, Southampton SO17 1BJ, UK. E-mail: G.Reid@soton.ac.uk*
[c]*GE Healthcare UK, White Lion Road, Amersham HP7 9LL, UK*

† Dedicated to the memory of Professor Ken Wade, FRS, in recognition of his many significant contributions to inorganic chemistry.

‡ Electronic supplementary information (ESI) available: X-ray structure of $[\subset Me_2N(CH_2)_2NMe(CH_2)_2]Cl$. CCDC 1053047–1053048 and 1053152-1053158. For ESI and crystallographic data in CIF or other electronic format see DOI: 10.1039/c5dt01120e

Open Access Article. Published on 20 April 2015. Downloaded on 11/26/2024 12:58:05 AM.
This article is licensed under a Creative Commons Attribution 3.0 Unported Licence.

cyclononane, L′) to form *fac*-[MF_3(L′)]·$x$$H_2O$ for each of aluminium, gallium and indium.[15] The compounds formed with Me_3-tacn were found to crystallise as tetrahydrates, and extensive hydrogen bonding interactions between the water molecules of crystallisation and the coordinated fluorides were observed.

An alternative method for the production of the metal-fluoro complexes is to first synthesise the metal chloride analogue and then perform a halide exchange reaction using reagents such as Me_3SiF or Me_3SnF. For example, [AlF_2(py)$_4$]Cl was successfully formed from the reaction of [$AlCl_3$(py)$_n$] (n = 1 to 3) with Me_3SiF in pyridine.[16]

The use of aluminium[15] and gallium[17] fluoride complexes incorporating ^{18}F as a radiolabel, has attracted much recent interest as diagnostic imaging agents for PET (positron emission tomography). Key to their potential clinical suitability is the ability to incorporate the short-lived ^{18}F isotope ($t_{1/2}$ = 110 min.) rapidly and cleanly in water; the resulting aluminium fluoride complexes are stable under physiological conditions,[15] while the gallium fluoride radio-product is stable in phosphate buffered saline (PBS) solution.[17] A fuller understanding of the coordination chemistry of these Group 13 fluorides is expected to contribute to advancing the design of the next generation of ^{18}F imaging agents.

Here we report on the systematic study of the preparation, spectroscopic and structural features of several series of complexes of the three Group 13 trifluorides with bi- and polydentate N-donor ligands, to explore the suitability of hydrothermal synthesis for other neutral ligands. The work also investigates the effect of replacing amine with neutral N-heterocyclic ligands, and introducing the *mer*-trifluoride geometry, rather than the *fac* geometry present in the [MF_3(R_3-tacn)] systems.

Experimental

The MF_3·$3H_2O$ (M = Al, Ga or In), $GaCl_3$, 2,2′-bipyridyl, 1,10-phenanthroline, 2,2′:6′,2″-terpyridyl, 4,4′,4″-tris-*t*-butyl,-2,2′:6′,2″-terpyridyl (^{t}Bu_3-terpy), and *N*,*N*,*N*′,*N*′,*N*″-pentamethyldiethylenetriamine (PMDTA), were obtained from Sigma-Aldrich or Alfa-Aesar and used as supplied. Solvents were dried by distillation prior to use, CH_2Cl_2 and CH_3CN from CaH_2, hexane and toluene from sodium, THF from sodium benzophenone ketyl, methanol from magnesium/diiodine. All preparations of chloro-complexes were performed under an atmosphere of dry N_2 using Schlenk techniques and spectroscopic samples were prepared in a dry, N_2-purged glove box. Hydrothermal preparations were conducted in a 23 mL Teflon reactor vessel placed in a Parr stainless steel bomb. ^1H NMR spectra were recorded in CD_3OD on a Bruker AVII 400 spectrometer and referenced to the residual proton resonance. $^{19}F\{^1H\}$ NMR spectra were recorded in CD_3OD on Bruker AVII 400 and DPX400 spectrometers, with $CFCl_3$ as external reference. ^{27}Al, ^{71}Ga and ^{115}In NMR spectra were recorded in CH_3OH/CD_3OD on a Bruker AVII 400 NMR spectrometer and were referenced to $[Al(OH_2)_6]^{3+}$, $[Ga(OH_2)_6]^{3+}$ and $[In(OH_2)_6]^{3+}$, respectively, in H_2O/D_2O at pH = 1. Infra-red spectra were recorded as Nujol mulls between CsI plates on a Perkin Elmer Spectrum100 spectrometer over the range 4000–200 cm^{-1}. Microanalyses were undertaken by London Metropolitan University.

[AlF_3(terpy)]·$3H_2O$

AlF_3·$3H_2O$ (0.100 g, 0.72 mmol) was suspended in freshly distilled water (7 mL) and terpy (0.169 g, 0.72 mmol) was then added. The suspension was transferred into a Teflon container and loaded into a stainless steel high pressure vessel (Parr) and heated to 180 °C for 15 h. The vessel was then allowed to cool. A pale yellow solution had formed, a small aliquot of which was retained to grow crystals. For the remaining reaction mixture the solvent was removed *in vacuo*, yielding a pale orange solid. Yield: 0.18 g, 70%. IR (Nujol, ν/cm^{-1}): 3370 (ν O–H), 1640 (δ H–O–H) 656, 631, 620 (Al–F). ^1H NMR (298 K): δ = 8.90 (d, J_{HH} 8.0 Hz, [2H], ArH,) 8.76 (d, J_{HH} 8.0 Hz, [2H], ArH), 8.54 (d, J_{HH} 8.0 Hz, [2H], ArH), 8.39 (t, J_{HH} 8.0 Hz, [2H], ArH), 8.28 (t, J_{HH} 8.0 Hz, [H], ArH), 7.83 (t, J_{HH} 6.0 Hz, [2H], ArH), 4.87 (s, H_2O). $^{19}F\{^1H\}$ NMR (298 K): δ = −162.0 (d, $^2J_{FF}$ 23 Hz, [2F]), −177.3 (t, $^2J_{FF}$ 23 Hz, [F]). ^{27}Al NMR (298 K): δ = 16.7 (br). Microanalyses on several batches, which were pure by spectroscopic analysis (including the single crystals), consistently gave H and N content as expected, but very variable (low) C content for this complex. Slow evaporation of the reaction solvent gave crystals suitable for X-ray diffraction.

[GaF_3(terpy)]·$3H_2O$

Method 1: Method as for [AlF_3(terpy)]·$3H_2O$ using GaF_3·$3H_2O$ (0.200 g, 1.11 mmol) and terpy (0.259 g, 1.11 mmol). Orange solid. Yield 0.366 g, 80%. Required for $C_{15}H_{17}F_3GaN_3O_3$ (414.0): C, 43.5; H, 4.1; N, 10.2. Found: C, 43.3; H, 4.0; N, 10.3%. IR (Nujol, ν/cm^{-1}): 3407 (ν O–H), 1644 (δ H–O–H), 548, 504, 490(sh) (Ga–F). ^1H NMR (298 K): δ = 9.04 (d, J_{HH} 8.0 Hz, [2H], ArH,) 8.80 (d, J_{HH} 8.0 Hz, [2H], ArH), 8.78 (d, J_{HH} 8.0 Hz, [2H], ArH), 8.64 (t, J_{HH} 8.0 Hz, [H], ArH), 8.49 (t, J_{HH} 8.0 Hz, [2H], ArH), 8.03 (t, J_{HH} 6.0 Hz, [2H], ArH), 4.87 (s, H_2O). $^{19}F\{^1H\}$ NMR (298 K): δ = −156.3 (s, [2F]), −189.7 (s, [F]); (183 K) δ = −154.5 (s, [2F]), −188.9 (s, [F]). Slow evaporation of the reaction solvent gave crystals suitable for X-ray diffraction.

Method 2: A suspension of [$GaCl_3$(terpy)] (0.06 g, 0.15 mmol) in anhydrous MeCN (5 mL) was treated with 0.45 mL (0.45 mmol) of a 1.0 M solution of [NBu_4]F in thf. Addition of the fluoride source resulted in the dissolution of the chloride precursor and the formation of a pale yellow solution. The mixture was stirred at room temperature for 1 h and then the volatiles were removed *in vacuo* to yield a yellow gum. This was dissolved in a minimum volume of CH_2Cl_2 (*ca.* 2 mL) and layered with hexane. A pale yellow precipitate formed overnight. Yield 0.042 g, 67%. Spectroscopic data matched that observed for Method 1 and recrystallisation from CH_2Cl_2/hexane yielded small crystals whose unit cell dimensions matched those of the crystals obtained *via* Method 1.

Method 3: [$GaCl_3$(terpy)] (0.020 g, 0.050 mmol) was suspended in anhydrous MeCN (5 mL). A solution of [K(2.2.2-

Open Access Article. Published on 20 April 2015. Downloaded on 11/26/2024 12:58:05 AM.
This article is licensed under a Creative Commons Attribution 3.0 Unported Licence.

crypt)]F (0.067 g, 0.150 mmol) in 3 mL anhydrous MeCN was added dropwise to the chloride precursor. Addition of the fluoride source resulted in the dissolution of the chloride precursor and the formation of a colourless solution. The mixture was stirred at room temperature for 1 h, then the volatiles were removed *in vacuo* to give a white solid containing both the expected fluoride complex and the [K(2.2.2-crypt)]Cl by-product. Spectroscopic data for the former matched that observed from Method 1. No further purification was undertaken.

$[\{Ga(terpy)F\}_2(\mu\text{-}F)_2][PF_6]_2\cdot 4H_2O$

$[GaF_3(terpy)]\cdot 3H_2O$ (0.013 g, 0.025 mmol) was dissolved in a mixture CH_3CN/H_2O (ratio 1 : 3, 1.5 mL) and added to $[NH_4][PF_6]$ (0.004 g, 0.025 mmol) in H_2O (1.5 mL). The reaction solution was left to evaporate slowly at room temperature, resulting in the formation of orange crystals suitable for single crystal X-ray diffraction. Required for $C_{30}H_{30}F_{16}Ga_2N_6O_4P_2$: C, 34.5; H, 2.9; N, 8.1. Found: C, 34.4; H, 2.9; N, 8.2%. $^{19}F\{^1H\}$ NMR (CD_3OD, 183 K): δ = −75.1 (d, $[PF_6]^-$), −156.4 (s, [2F]), −189.8 (s, [F]).

$[InF_3(terpy)]\cdot 3H_2O$

Method as for $[AlF_3(terpy]\cdot 3H_2O$ using $InF_3\cdot 3H_2O$ (0.100 g, 0.44 mmol) and terpy (0.1032 g, 0.44 mmol). Pale orange solid. Yield: 0.10 g, 49%. Required for $C_{15}H_{17}F_3InN_3O_3$ (459.1): C, 39.2; H, 3.7; N, 9.2. Found: C, 39.4; H, 3.9; N, 9.3%. IR (Nujol, ν/cm^{-1}): 3490, 3400(ν O–H), 1654 (δ H–O–H), 476, 427, 406 (In–F). ^{1}H NMR (298 K): δ = 8.68 (m, [2H], ArH), 8.61 (d, J_{HH} 8.0 Hz, [2H], ArH), 8.39 (d, J_{HH} 8.0 Hz, [2H], ArH), 8.07–7.97 (m, [3H], ArH), 7.47 (m, [2H], ArH), 4.87 (s, H_2O). $^{19}F\{^1H\}$ NMR (298 K): δ = −157.8 (br s [2F]), −181.6 (br s [F]); (183 K): −157.5 (br s [2F]), −178.5 (br s [F]).

$[AlF_3(bipy)(OH_2)]\cdot 2H_2O$

Method as for $[AlF_3(terpy)]\cdot 3H_2O$ using $AlF_3\cdot 3H_2O$ (0.200 g, 1.45 mmol) and bipy (0.226 g, 1.45 mmol). The resulting pale pink solid was washed with acetonitrile and filtered to leave a white solid which was dried *in vacuo*. Yield: 0.20 g, 47%. Required for $C_{10}H_{14}AlF_3N_2O_3$ (294.2): C, 40.8; H, 4.8; N, 9.5. Found: C, 40.6; H, 4.6; N, 9.7%. IR (Nujol, ν/cm^{-1}): 3533, 3422 (ν O–H), 1689 br (δ H–O–H), 610, 590(sh) (Al–F). ^{1}H NMR (CD_3OD, 298 K): δ = 9.04 (d, J_{HH} 4.0 Hz, [1H], ArH), 8.76 (d, J_{HH} 4.4 Hz, [1H], ArH), 8.59 (d, J_{HH} 7.6 Hz, [1H], ArH), 8.44 (d, J_{HH} 8.1 Hz, [1H], ArH), 8.33 (t, J_{HH} 7.7 Hz, [1H], ArH), 8.14 (t, J_{HH} 7.5 Hz, [1H], ArH), 7.81–7.85 (m, [1H], ArH), 7.63 (t, J_{HH} 5.9 Hz, [1H], ArH), 4.75 (s, H_2O). $^{19}F\{^1H\}$ NMR (298 K): δ = −172.8 (br s); (183 K): −162.3 (s, [F]), −176.4 (s, [2F]). ^{27}Al NMR (298 K): δ = 8.3 (br s, $w_{1/2}$ = 400 Hz), resonance lost on cooling below 233 K. Slow evaporation of the reaction solvent gave crystals suitable for X-ray diffraction.

$[GaF_3(bipy)(OH_2)]\cdot 2H_2O$

Method as for $[AlF_3(terpy)]\cdot 3H_2O$ using $GaF_3\cdot 3H_2O$ (0.200 g, 1.11 mmol) and bipy (0.158 g, 1.11 mmol). Pale pink solid. Yield 0.314 g, 84%. Required for $C_{10}H_{14}F_3GaN_2O_3$ (337.0): C, 35.7; H, 4.1; N, 8.3. Found: C, 35.6; H, 4.1; N, 8.2%. IR (Nujol, ν/cm^{-1}): 3500, 3380 (ν O–H), 1660 br (δ H–O–H), 527, 473 (Ga–F). ^{1}H NMR (CD_3OD, 298 K): δ = 9.07 (br, [2H], ArH), 8.66 (d, J_{HH} 8 Hz, [2H], ArH), 8.37 (t, J_{HH} ∼ 8 Hz, [2H], ArH), 7.89 (s, [2H], ArH); (183 K): 9.09 (s, [2H]), 8.81 (br, s [2H], ArH), 8.47 (s, [2H]), 7.97 (s, [2H]), 4.75 (s, H_2O). $^{19}F\{^1H\}$ NMR (298 K): δ = −176.2 (br s); (183 K): −160.9 (s, [F]), −181.5 (s, [2F]). Slow evaporation of the reaction solvent gave crystals suitable for X-ray diffraction.

$[InF_3(bipy)(OH_2)]\cdot 2H_2O$

Method as for $[AlF_3(terpy)]\cdot 3H_2O$ using $InF_3\cdot 3H_2O$ (0.200 g, 0.89 mmol) and bipy (0.138 g, 0.89 mmol), yielding a pale yellow solid. Yield: 0.17 g, 50%. Required for $C_{10}H_{14}F_3InN_2O_3$ (382.1): C, 31.4; H, 3.7; N, 7.3. Found: C, 31.6; H, 3.6; N, 7.4%. IR (Nujol, ν/cm^{-1}): 3422 br (ν O–H), 1655 br (δ H–O–H), 442, 428, 404 (In–F). ^{1}H NMR (CD_3OD, 298 K): δ = 8.78 (br s, [2H], ArH), 8.68 (br s, [2H], ArH), 8.45 (br s, [2H], ArH), 7.96 (br s, [2H], ArH), 4.75 (s, H_2O); (183 K): 8.99 (br, s), 8.95 (br s,), 8.66 (s), 8.52 (vbr), 8.05–7.99 (m). $^{19}F\{^1H\}$ NMR (CD_3OD, 298 K): not observed; (183 K): δ = −152.9 (s, [F]), −178.1 (s, [2F]).

$[AlF_3(phen)(OH_2)]$

Method as for $[AlF_3(terpy)(OH_2)]\cdot 2H_2O$, but using $AlF_3\cdot 3H_2O$ (0.200 g, 1.45 mmol) and phen (0.261 g, 1.45 mmol). White solid. Yield: 0.254 g, 62%. Required for $C_{12}H_{10}AlF_3N_2O$ (282.2): C, 51.1; H, 3.6; N, 9.9. Found: C, 50.9; H, 3.4; N, 10.0%. IR (Nujol, ν/cm^{-1}): 3200br (ν O–H), 1670 (δ H–O–H), 637, 608 (Al–F). ^{1}H NMR (298 K): δ = 9.30 (d, J_{HH} 5.1 Hz, [1H], ArH), 9.17 (d, J_{HH} 3.7 Hz, [1H], ArH), 8.88 (d, J_{HH} 7.6 Hz, [1H], ArH), 8.66 (d, J_{HH} 8.8 Hz, [1H], ArH), 8.25 (s, [1H], ArH), 8.14 (m, [1H], ArH), 8.09 (s, [1H], ArH), 7.93 (m, J_{HH} 4.2 Hz, [1H], ArH), 4.75 (s, H_2O). $^{19}F\{^1H\}$ NMR (298 K): δ = −157.3 (br s [F]), −174.8 (s, [2F]); (183 K): δ = −162.5 (br s [F]), −177.3 (s, [2F]);. ^{27}Al NMR (298 K): δ = 8.8 (br s, $w_{1/2}$ 450 Hz).

$[GaF_3(phen)(OH_2)]$

Method as for $[AlF_3(terpy)]\cdot 3H_2O$, using $GaF_3\cdot 3H_2O$ (0.200 g, 1.11 mmol) and phen (0.200 g, 1.11 mmol). Pale red solid. Yield 0.315 g, 79%. Required for $C_{12}H_{10}F_3GaN_2O$ (324.9): C, 44.4; H, 3.1; N, 8.6. Found: C, 44.4; H, 3.1; N, 8.5%. IR (Nujol, ν/cm^{-1}): 3200 br (ν O–H), 1680 (δ H–O–H), 560, 543, 511 (Ga–F). ^{1}H NMR (298 K): δ = 9.34 (d, J_{HH} 4 Hz, [2H], ArH), 8.89 (d, J_{HH} 12 Hz, [2H], ArH), 8.26 (s, [2H], ArH), 8.15 (br, [2H], ArH) 4.87 (s, H_2O); (183 K): 9.34 (s), 9.02 (d), 8.94 (d), 8.33–8.21 (m). $^{19}F\{^1H\}$ NMR (298 K): δ = −152 (br s [F]), −176 (br, [2F]); (183 K): δ = −151.0 (br s [F]), −184.0 (s, [2F]). Slow evaporation of the reaction solvent gave crystals suitable for X-ray diffraction.

$[InF_3(phen)(OH_2)]$

Method as for $[AlF_3(terpy)]\cdot 3H_2O$, but using $InF_3\cdot 3H_2O$ (0.200 g, 0.89 mmol) and phen (0.160 g, 0.89 mmol). Pale orange solid. Yield: 0.16 g, 49%. Required for $C_{12}H_{10}F_3InN_2O$ (370.0): C, 39.0; H, 2.7; N, 7.6. Found: C, 39.2; H, 2.8; N, 7.7%. IR (Nujol, ν/cm^{-1}): 3360 br, 3177 (ν O–H), 1660 w (δ H–O–H), 446, 422 br, 405(sh) (In–F). ^{1}H NMR (298 K): δ = 9.30 (br s,

Open Access Article. Published on 20 April 2015. Downloaded on 11/26/2024 12:58:05 AM.
This article is licensed under a Creative Commons Attribution 3.0 Unported Licence.

[1H], ArH), 9.02–8.96 (br [3H], ArH), 8.29–8.07 (br, m, [4H], ArH), 4.87 (s, H_2O); (183 K): 9.28 (s), 8.98 (s), 8.76 (s), 8.33–8.22 (m), 7.95 (m). $^{19}F\{^1H\}$ NMR (298 K): not observed; (183 K): δ = −157 (br, [F]), −199 (br, [2F]).

[$GaCl_3$(terpy)]

A solution of terpy (0.258 g, 1.11 mmol) in anhydrous CH_2Cl_2 (5 mL) was added dropwise to a solution of $GaCl_3$ (0.195 g, 1.11 mmol) in 5 mL anhydrous CH_2Cl_2. A white precipitate formed upon addition of the ligand. The mixture was stirred at room temperature for 1 h. The product was isolated by filtration, washed with hexane and dried *in vacuo*. White solid. Yield: 0.402 g, 88%. Required for $C_{15}H_{11}Cl_3GaN_3$: C, 44.0; H, 2.7; N, 10.3. Found: C, 43.5; H, 2.6; N, 10.1%. IR (Nujol, ν/cm^{-1}): 267 s, 254 br, (Ga–Cl). ^1H NMR (CD_3CN, 298 K): δ = 9.06–9.04 (m, [2H], ArH), 8.75–8.73 (m, [3H], ArH), 8.67–8.65 (m, [2H], ArH), 8.53–8.49 (m, [2H], ArH), 8.08–8.05 (m, [2H], ArH).

[$GaCl_3$($^tBu_3$-terpy)]

A solution of $^tBu_3$-terpy (0.111 g, 0.278 mmol) in anhydrous CH_2Cl_2 (5 mL) was added dropwise to a solution of $GaCl_3$ (0.025 g, 0.139 mmol) in anhydrous CH_2Cl_2 (5 mL). Addition of the ligand resulted in the formation of a white precipitate. The mixture was stirred at room temperature for 1 h. The solid was isolated by filtration, washed with a further 10 mL CH_2Cl_2 and dried *in vacuo*. White solid. Yield 0.062 g, 77%. Required for $C_{27}H_{35}Cl_3GaN_3{\cdot}CH_2Cl_2$ (662.60): C, 50.7; H, 5.6; N, 6.3. Found: C, 50.4; H, 5.6; N, 6.5%. ^1H NMR (CD_3CN, 298 K): δ = 1.42 (s, [18H], ^tBu), 1.44 (s, [9H], ^tBu), 7.47–7.46 (br m, [2H], ArH), 8.50 (br s, [2H], ArH), 8.61–8.60 (br m, [2H], ArH), 8.77 (br s, [2H], ArH).

The same reaction performed in a 1 : 1 stoichiometric ratio gave a spectroscopically identical product. However, crystals formed from the filtrate gave the ionic by-product [$GaCl_2$($^tBu_3$-terpy)][$GaCl_4$]·CH_2Cl_2.

[⊂$Me_2N(CH_2)_2NMe(CH_2)_2]_2[Al_2F_8(OH_2)_2]$·$2H_2O$

Method as for [AlF_3(bipy)(OH_2)]·$2H_2O$, but using $AlF_3{\cdot}3H_2O$ (0.200 g, 1.45 mmol) and PMDTA (0.3 mL, 1.45 mmol). A brown gum was obtained after removing the solvent. This was washed with MeCN, producing a white powder. Yield: 0.44 g, 58%. Required for $C_{14}H_{42}Al_2F_8N_4O_4$ (536.4): C, 31.4; H, 7.8; N, 10.4. Found: C, 31.3; H, 7.8; N, 10.4%. IR (Nujol, ν/cm^{-1}): 3370 br (ν O–H), 1673 (δ H–O–H), 616 br, 569 br, (Al–F). ^1H NMR (CD_3CN, 298 K): δ = 4.87 (s, H_2O), 3.35 (t, J_{HH} 6.0 Hz, [4H], CH_2), 3.07 (s, [6H], Me), 2.67 (br s, [4H], CH_2CH_2), 2.32 (s, [3H], Me). $^{19}F\{^1H\}$ NMR (CD_3CN, 298 K): δ = −194.6 (6 lines $^1J_{AlF}$ = 38 Hz). ^{27}Al NMR (CH_3CN, 298 K): δ = 48.7 (s). Slow evaporation of the reaction solvent gave crystals suitable for X-ray diffraction.

The corresponding gallium and indium fluoride reactions were conducted similarly.

[⊂$Me_2N(CH_2)_2NMe(CH_2)_2]_2[Ga_2F_8(OH_2)_2]$·$2H_2O$

Required for $C_{14}H_{42}F_8Ga_2N_4O_4$ (619.9): C, 27.0; H, 6.8; N, 9.0. Found: C, 26.7; H, 6.4; N, 9.8%. ^1H NMR (CD_3CN, 298 K): δ = 4.87 (s, H_2O), 3.35 (t, J_{HH} 6.0 Hz, [4H], CH_2), 3.07 (s, [6H], Me), 2.67 (br s, [4H], CH_2CH_2), 2.32 (s, [3H], Me). $^{13}C\{^1H\}$ NMR (CD_3CN): δ = 44.18 (s), 44.84 (s), 48.04 (s), 61.59 (s). IR (Nujol, ν/cm^{-1}): 3420 br (ν O–H), 1673 (δ H–O–H), 518 br, 477 br, (Ga–F).

A small number of crystals obtained from the Ga and In reaction mixtures were found to be [⊂$Me_2N(CH_2)_2NMe(CH_2)_2$]Cl (see text and ESI‡).

X-Ray experimental

Details of the crystallographic data collection and refinement parameters are given in Table 1. Crystals suitable for single crystal X-ray analysis were obtained as described above. Data collections used a Rigaku AFC12 goniometer equipped with an enhanced sensitivity (HG) Saturn724+ detector mounted at the window of an FR-E+ SuperBright molybdenum (λ = 0.71073 Å) rotating anode generator with VHF Varimax optics (70 μm focus) with the crystal held at 100 K (N_2 cryostream). Structure solution and refinements were performed with either SHELX (S/L)97 or SHELX(S/L)2013[18] and were straightforward, except where detailed below. H atoms bonded to C were placed in calculated positions using the default C–H distance and refined using a riding model. In the case of the [AlF_3(bipy)(OH_2)]·$2H_2O$ structure, the H-atoms on the co-crystallised water molecules were not located in the difference map. While not included in the refinement, the H-atoms are inferred from the H-bonding distances of F···O and O···O and are thus included in the formulae. The H-atoms on both the coordinated and co-crystallised water molecules could not be located in the structure of [⊂$Me_2N(CH_2)_2NMe(CH_2)_2]_2[Al_2F_8(OH_2)_2]$·$2H_2O$. While not included in the refinement, the H-atoms are similarly inferred and included in the formulae. CCDC numbers 1053047–1053048 and 1053152–1053158.

Results and discussion

The unreactive and poorly soluble nature of the $MF_3{\cdot}3H_2O$ makes reaction with neutral ligands in organic solvents difficult or impossible. We therefore used the hydrothermal approach (180 °C/15 h) and found this gave high yields of [MF_3(terpy)]·$3H_2O$ (below). The same approach was then extended to reactions with *N*,*N*,*N*′,*N*′,*N*″-pentamethyldiethylenetriamine (PMDTA), and to the diimines, 2,2′-bipyridyl and 1,10-phenanthroline.

[MF_3(terpy)]·$3H_2O$ (M = Al, Ga or In)

The reaction of the $MF_3{\cdot}3H_2O$ with terpy in a 1 : 1 molar ratio in water at 180 °C/15 h, followed by removal of the solvent *in vacuo* at room temperature, gave high yields of the [MF_3(terpy)]·$3H_2O$ as pale orange solids. Slow evaporation of a small portion of the mother liquor at ambient temperatures gave crystals of [MF_3(terpy)]·$3H_2O$ (M = Al or Ga). For M = Al, the structure shows (Fig. 1) a distorted octahedral geometry about the aluminium, the distortions being largely due to the rigid terpy ligand which results in N–Al–N angles significantly less

 This journal is © The Royal Society of Chemistry 2015

Open Access Article. Published on 20 April 2015. Downloaded on 11/26/2024 12:58:05 AM.
This article is licensed under a Creative Commons Attribution 3.0 Unported Licence.

Table 1 Crystallographic parameters[a]

Compound	$[AlF_3(terpy)]\cdot 3H_2O$	$[GaF_3(terpy)]\cdot 3H_2O$	$[AlF_3(bipy)(OH_2)]\cdot 2H_2O$	$[GaF_3(bipy)(OH_2)]\cdot 2H_2O$
Formula	$C_{15}H_{17}AlF_3N_3O_3$	$C_{15}H_{17}F_3GaN_3O_3$	$C_{10}H_{14}AlF_3N_2O_3$	$C_{10}H_{14}F_3GaN_2O_3$
M	371.30	414.04	294.20	336.95
Crystal system	Monoclinic	Monoclinic	Monoclinic	Monoclinic
Space group (no.)	$P2_1/c$ (14)	$P2_1/c$ (14)	$P2_1/n$ (14)	$P2_1/n$ (14)
a/Å	9.4806(9)	10.323(5)	8.976(5)	9.056(3)
b/Å	25.104(2)	9.708(5)	7.300(5)	7.371(2)
c/Å	7.0846(6)	16.131(5)	19.062(5)	18.904(6)
α/°	90	90	90	90
β/°	104.425(7)	100.484(5)	93.331(5)	93.462(6)
γ/°	90	90	90	90
U/Å^3	1633.0(3)	1589.6(12)	1246.9(11)	1259.6(7)
Z	4	4	4	4
μ(Mo-K$_\alpha$)/mm^{-1}	0.177	1.785	0.207	2.228
F(000)	768	840	608	680
Total number reflections	6803	9623	8257	11 425
R_{int}	0.062	0.048	0.078	0.154
Unique reflections	2163	3646	2848	2883
No. of parameters, restraints	294,0	250, 0	188, 0	196, 8
R_1, wR_2 [$I > 2\sigma(I)$][b]	0.071, 0.133	0.037, 0.084	0.060, 0.144	0.048, 0.130
R_1, wR_2 (all data)	0.146, 0.172	0.056, 0.089	0.104, 0.168	0.051, 0.132

Compound	$[GaF_3(phen)\text{-}(OH_2)]$	$[GaCl_2(^tBu_3\text{-terpy})]\text{-}[GaCl_4]\cdot CH_2Cl_2$	$[\subset Me_2N(CH_2)_2NMe\text{-}(CH_2)_2]_2[Al_2F_8(OH_2)_2]\cdot 2H_2O$	$[\{Ga(terpy)F\}_2(\mu\text{-}F)_2]\text{-}[PF_6]_2\cdot 4H_2O$
Formula	$C_{12}H_{10}F_3GaN_2O$	$C_{14}H_{18.5}Cl_4GaN_{1.5}$	$C_{14}H_{42}Al_2F_8N_4O_4$	$C_{30}H_{30}F_{16}Ga_2N_6O_4P_2$
M	324.94	419.32	538.4	1043.98
Crystal system	Monoclinic	Triclinic	Monoclinic	Triclinic
Space group (no.)	$P2_1/n$ (14)	$P\bar{1}$ (2)	$C2/c$ (15)	$P\bar{1}$ (2)
a/Å	8.3906(5)	11.674(3)	24.054(10)	9.774(2)
b/Å	7.1940(5)	12.642(4)	7.558(3)	10.460(2)
c/Å	19.0124(13)	13.756(5)	16.389(7)	10.646(2)
α/°	90	89.137(17)	90	78.064(12)
β/°	100.631(3)	78.682(16)	123.374(4)	62.736(8)
γ/°	90	65.276(15)	90	85.448(14)
U/Å^3	1127.93(13)	1803.1(11)	2488.3(17)	946.5(3)
Z	4	4	6	1
μ(Mo-K$_\alpha$)/mm^{-1}	2.472	2.111	0.214	1.633
F(000)	648	848	1200	520
Total number reflections	12 632	16 476	5785	17 446
R_{int}	0.051	0.141	0.035	0.079
Unique reflections	2581	7870	2822	3925
No. of parameters, restraints	178, 2	379, 0	170, 6	271, 0
R_1, wR_2 [$I > 2\sigma(I)$][b]	0.025, 0.064	0.086, 0.192	0.078, 0.212	0.043, 0.109
R_1, wR_2 (all data)	0.028, 0.066	0.125, 0.211	0.098, 0.231	0.049, 0.111

[a] Common items: T = 100 K; wavelength (Mo-Kα) = 0.71073 Å; θ(max) = 27.5°. [b] $R_1 = \sum||F_o| - |F_c||/\sum|F_o|$; w$R_2 = [\sum w(F_o^2 - F_c^2)^2/\sum wF_o^2]^{1/2}$.

than 90°/180°, whereas the F–Al–F and (*cis*) F–Al–N angles are close to those expected for an octahedron.

There is extensive H-bonding between the fluoride ligands and the lattice water molecules (Fig. 2), as well as π-stacking of the aromatic rings (Fig. 3).

The Al–F bond lengths are very similar to those observed in *fac*-$[AlF_3(Me_3\text{-tacn})]\cdot 4H_2O$,[15] but the Al–N bonds are shorter by ~0.05 Å, suggesting the macrocyclic ring may limit the close approach of the N atoms to the metal centre. The molecular structure of $[GaF_3(terpy)]\cdot 3H_2O$ is very similar to that of the Al(III) complex (Fig. 4) with the Ga–F bonds *ca.* 0.1 Å longer than the corresponding Al–F, whilst the Ga–N and Al–N are little different.

As found in the aluminium complex, the structure of $[GaF_3(terpy)]\cdot 3H_2O$ shows extensive H-bonding as shown in Fig. 5 as well as π-stacking interactions of 3.57 and 3.62 Å (see ESI Fig. S1‡), although the arrangements differ in detail. The Ga–F distances are very similar to those found in *fac*-$[GaF_3(Me_3\text{-tacn})]\cdot 4H_2O$.[15] The Ga–N distances are also not significantly different to those found in the $[GaX_3(terpy)]$ (X = Cl or Br),[19] although the extensive H-bonding in the fluoride complex is absent in the structures of the heavier halides. The single bond covalent radii of Al(III) and Ga(III) are quoted in standard texts as nearly identical (~1.25 Å), although the ionic radius of Ga^{3+} is ~0.07 Å larger than that of Al^{3+}.[20] The limited number of structurally characterised complexes of the trifluorides limits detailed comparisons, but it seems that the metal-donor bond length may be very sensitive to the electronegativity of the donor atom, with little difference between Al–L

Open Access Article. Published on 20 April 2015. Downloaded on 11/26/2024 12:58:05 AM.
This article is licensed under a Creative Commons Attribution 3.0 Unported Licence.

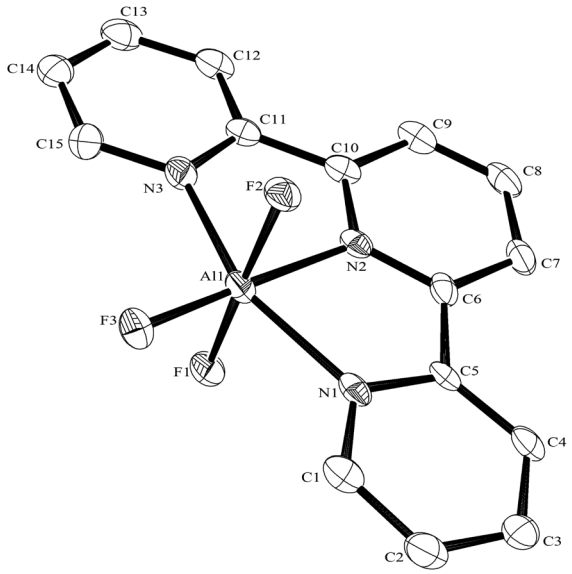

Fig. 1 The structure of the Al species in $[AlF_3(terpy)]\cdot 3H_2O$ with ellipsoids drawn at the 50% probability level. Hydrogen atoms on terpy are omitted for clarity. Selected bond lengths (Å) and angles (°) are Al1–F1 = 1.761(2), Al1–F2 = 1.762(2), Al1–F3 = 1.737(2), Al1–N1 = 2.057(3), Al1–N2 = 2.010(3), Al1–N3 = 2.059(3), F1–Al1–F3 = 92.55(12), F2–Al1–F3 = 91.08(11), F1–Al1–F2 = 176.34(13), N1–Al1–N2 = 77.58(13), N2–Al1–N3 = 78.17(13), N1–Al1–N3 = 155.73(13).

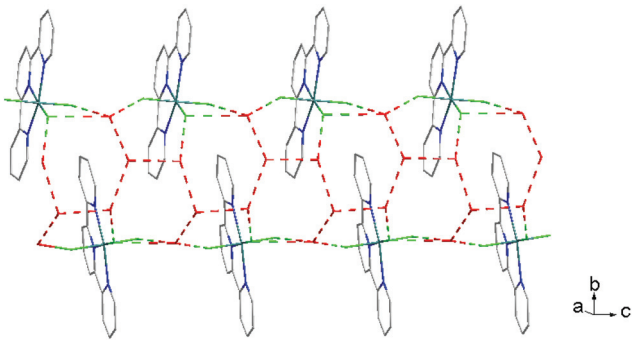

Fig. 2 The H-bonding network (red) in the crystals of $[AlF_3(terpy)]\cdot 3H_2O$.

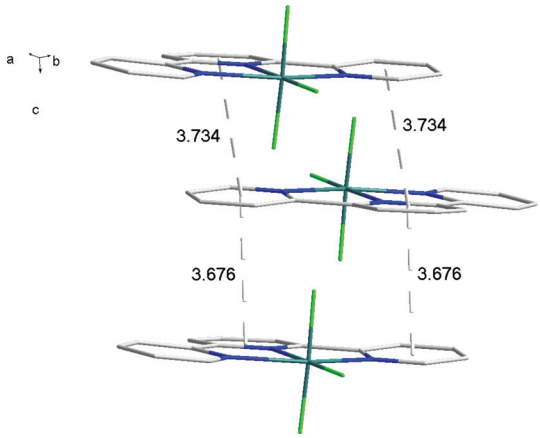

Fig. 3 π-stacking in the structure of $[AlF_3(terpy)]\cdot 3H_2O$ with lattice water omitted for clarity.

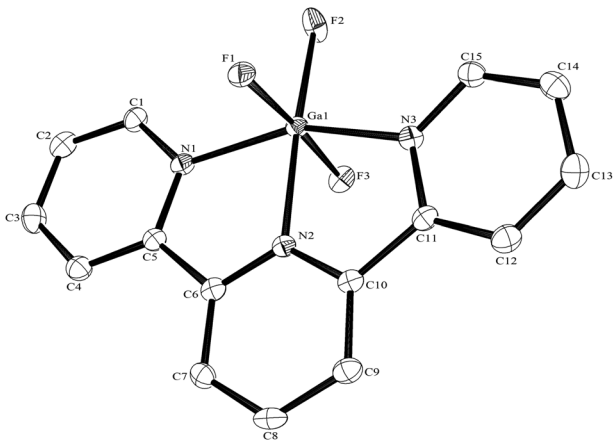

Fig. 4 The structure of the Ga species in $[GaF_3(terpy)]\cdot 3H_2O$ with ellipsoids drawn at the 50% probability level. Hydrogen atoms are omitted for clarity. Selected bond lengths (Å) and angles (°):Ga1–F1 = 1.8781(17), Ga1–F2 = 1.8780(16), Ga1–F3 = 1.8895(17), Ga1–N1 = 2.082(2), Ga1–N2 = 2.045(2), Ga1–N3 = 2.093(2), F1–Ga1–F2 = 92.12(7), F2–Ga1–F3 = 90.60(7), F1–Ga1–F3 = 176.29(7), N1–Ga1–N2 = 77.21(8), N2–Ga1–N3 = 77.26(9), N1–Ga1–N3 = 154.28(8).

and Ga–L with heavier donor ligands and halides,[21] but significant differences in the M–F bond lengths. The effects of solvent molecules and hydrogen bonding also complicates the interpretation of small differences in metal-donor bond lengths,[19,22] and these may be a significant factor in the extensively hydrogen bonded metal fluoride complexes.

Interpretation of the spectroscopic properties (Experimental section) of the three terpy complexes is straightforward. The IR spectra show strong, very broad features due to the ν(OH) and δ(HOH) modes of the water and three ν(MF) stretches, as expected for a *mer*-trifluoride (theory $2A_1 + B_1$). The ^{1}H NMR spectra in CD_3OD exhibit sharp multiplet resonances for the terpy protons and a broad signal for the water, whilst the $^{19}F\{^1H\}$ NMR spectra show two resonances in a 2 : 1 ratio due to F_{transF} and F_{transN} respectively. The $^{19}F\{^1H\}$ resonances for the $[AlF_3(terpy)]$ show doublet and triplet $^2J_{FF}$ couplings of 23 Hz, but for the gallium and indium complexes only broad singlets are observed over the temperature range 298–183 K.[23] The aluminium complex also exhibited a ^{27}Al NMR resonance at δ = 16.7 as a broad singlet with no resolved $^1J_{AlF}$ coupling, which is in the range expected for six-coordinate aluminium.[24] Neither the gallium nor indium complex exhibited a metal nucleus resonance, probably due to fast quadrupolar relaxation. The multinuclear NMR data show that the molecular structures of these complexes are maintained in MeOH solution.

 This journal is © The Royal Society of Chemistry 2015

Open Access Article. Published on 20 April 2015. Downloaded on 11/26/2024 12:58:05 AM.
This article is licensed under a Creative Commons Attribution 3.0 Unported Licence.

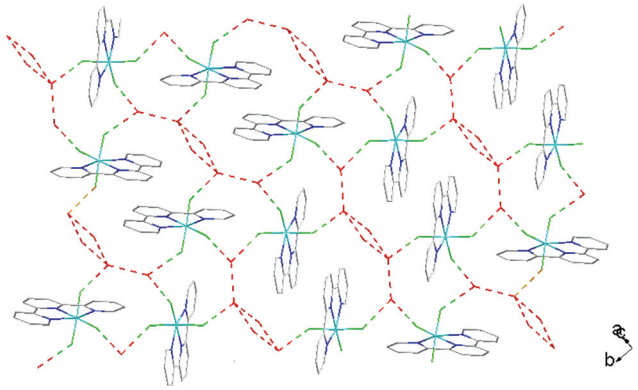

Fig. 5 View showing the H-bonding network (red) in $[GaF_3(terpy)]\cdot 3H_2O$.

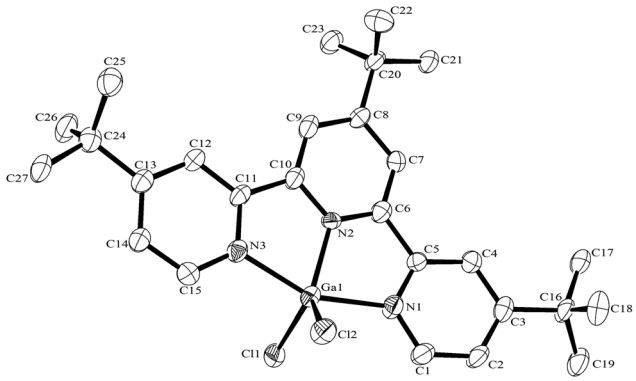

Fig. 6 The structure of the cation in $[GaCl_2(^tBu_3\text{-terpy})][GaCl_4]$ with ellipsoids drawn at the 50% probability level. Hydrogen atoms are omitted for clarity. Selected bond lengths (Å) and angles (°): Ga1–N1 = 2.092(5), Ga1–N2 = 1.995(5), Ga1–N3 = 2.066(5), Ga1–Cl1 = 2.195(2), Ga1–Cl2 = 2.169(2), N2–Ga1–N3 = 77.9(2), N1–Ga1–N2 = 77.3(2), N1–Ga1–N3 = 155.1(2), N2–Ga1–Cl2 = 125.68(18), N3–Ga1–Cl2 = 97.76(17), N1–Ga1–Cl2 = 95.78(17), N2–Ga1–Cl1 = 120.20(18), N3–Ga1–Cl1 = 96.80(16), N1–Ga1–Cl1 = 96.56(18), Cl1–Ga1–Cl2 = 114.10(8).

The synthesis of the $[GaF_3(terpy)]$ by halide exchange was also explored. The $[GaCl_3(terpy)]$ precursor was made in high yield by reaction of $GaCl_3$ with terpy in anhydrous CH_2Cl_2 solution, and its composition confirmed by microanalysis and spectroscopically. Complete fluorination of $[GaCl_3(terpy)]$ in MeCN solution was achieved at room temperature with $[^nBu_4N]F$ in thf or [K(2.2.2-crypt)]F in MeCN; the $[GaF_3(terpy)]$ produced was spectroscopically identical to samples produced by the hydrothermal route, and crystals obtained using the $[^nBu_4N]F$ route had the same unit cell. Fluorination with [K(2.2.2-crypt)]F was also successful at 80 °C in MeCN, confirming the gallium species is thermally stable under these conditions. The $[GaCl_3(terpy)]$ was relatively poorly soluble in organic solvents and in an attempt to increase the solubility, the corresponding complex of 4,4′,4″-tris-*t*-butyl,-2,2′:6′,2″-terpyridyl, $[GaCl_3(^tBu_3\text{-terpy})]$, was prepared. Its properties were very similar to the terpy complex (Experimental section), but it was in fact rather less soluble in common organic solvents. However, crystals grown from the filtrate from one synthesis were found to be $[GaCl_2(^tBu_3\text{-terpy})][GaCl_4]\cdot CH_2Cl_2$, containing a five-coordinate cation. This minor by-product probably results from the presence of a small excess of $GaCl_3$ in the synthesis, which extracts a chloride from the neutral species to form the stable $[GaCl_4]^-$ anion. The structure of the cation is shown in Fig. 6. The geometry is a distorted trigonal bipyramid with apical N, distorted by the steric constraints of the $^tBu_3$-terpy (N3–Ga1–N1 = 155.1(2)°), as also found in the neutral $[GaCl_3(terpy)]$ complex above. Comparisons of the bond lengths between $[GaCl_2(^tBu_3\text{-terpy})]^+$ and $[GaCl_3(terpy)]$,[19] as expected, show shorter bonds in the five-coordinate cation (Ga–Cl = 2.169(2), 2.195(2), Ga–N = 1.995(5)–2.092(5) Å) compared to the six-coordinate neutral complex (Ga–Cl = 2.2511(5)–2.4118(6), Ga–N = 2.0412(5)–2.1024(15) Å).

$[\{Ga(terpy)F\}_2(\mu\text{-}F)_2][PF_6]_2\cdot 4H_2O$

The *fac*-$[GaF_3(BzMe_2\text{-tacn})]$ has been shown to function as a neutral 'metalloligand' through the coordinated fluorides towards alkali metal and ammonium cations in aqueous solution, leading to supramolecular arrays with Ga–F–M linkages,[25] whilst combination of Gd^{3+} and *fac*-$[GaF_3(Me_3\text{-tacn})]$ leads to '$[Gd_3Ga_2]$' cores that are of interest as molecular magnets.[26] A key feature of these systems is that the three *facial* Ga–F bonds remain intact throughout. To explore if the *meridional* trifluoride arrangement present in $[GaF_3(terpy)]$ could function in a similar manner, a H_2O-MeCN solution containing $[GaF_3(terpy)]$ and $[NH_4][PF_6]$ was allowed to evaporate slowly. Orange crystals formed and an X-ray structure analysis on these showed that rather than forming an ammonium-metalloligand complex, the dimer, $[\{Ga(terpy)F\}_2(\mu\text{-}F)_2][PF_6]_2\cdot 4H_2O$ had formed.

The centrosymmetric cation (Fig. 7) contains six-coordinate gallium, severely distorted from regular octahedral by the steric constraints of the terpy ligand (N1–Ga1–N3 = 153.85(10)°), and the fluoride bridges are asymmetric (Ga1–F1 = 1.889(2), Ga1–F1a = 2.003(2) Å). There is extensive hydrogen bonding linking the lattice water molecules, the cations and the $[PF_6]^-$ anions (Fig. 8). The complex, formed by dissociation of one fluoride from each gallium centre, followed by dimerisation, dissolves in CD_3OD with decomposition and formation of a white precipitate. The $^{19}F\{^1H\}$ NMR spectrum of the supernatant shows only $[GaF_3(terpy)]$ and $[PF_6]^-$ as significant species.

$[MF_3(diimine)(OH_2)]\cdot nH_2O$

The hydrothermal method also proved a suitable route to obtain $[MF_3(bipy)(OH_2)]\cdot 2H_2O$ and $[MF_3(phen)(OH_2)]$ in good yields. The structures of $[InF_3(phen)(OH_2)]$ and $[InF_3(bipy)(OH_2)]\cdot 2H_2O$ obtained from samples made from aqueous HF solution have been reported previously.[13] The $[MF_3(bipy)(OH_2)]\cdot 2H_2O$ (M = Al or Ga) are monoclinic, $P2_1/n$, with six-coordinate metal centres and a *mer*-fluoride arrangement,

Open Access Article. Published on 20 April 2015. Downloaded on 11/26/2024 12:58:05 AM.
This article is licensed under a Creative Commons Attribution 3.0 Unported Licence.

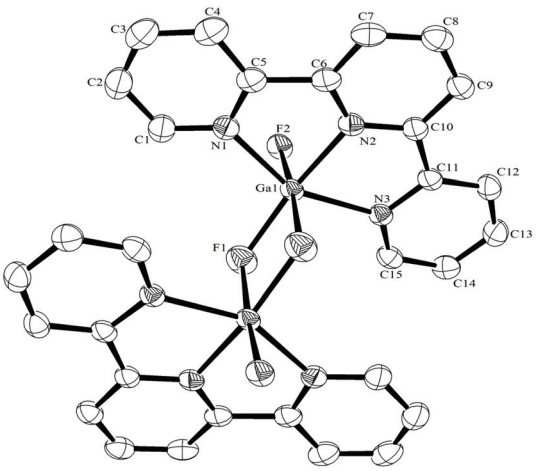

Fig. 7 The structure of the centrosymmetric cation in $[\{Ga(terpy)F\}_2(\mu\text{-}F)_2][PF_6]_2\cdot 4H_2O$ with ellipsoids drawn at the 50% probability level. Hydrogen atoms are omitted for clarity. Selected bond lengths (Å) and angles (°): Ga1–F2 = 1.8564(17), Ga1–F1 = 1.889(2), Ga1–F1a = 2.003(2), Ga1–N2 = 2.026(2), Ga1–N1 = 2.095(3), Ga1–N3 2.110(2), F2–Ga1–F1 = 98.39(8), F2–Ga1–F1a = 174.58(7), F1–Ga1–F1a = 76.19(9), F2–Ga1–N2 = 97.02(8), F1–Ga1–N2 = 88.40(9), F2–Ga1–N1 = 88.84(9), F1a–Ga–N1 = 102.47(9), F1–Ga1–N1 = 92.37(9), N2–Ga1–N1 = 77.26(10), F2–Ga1–N3 = 88.19(8), F1a–Ga1–N3 = 103.67(9), F1–Ga1–N3 = 93.03(9), N2–Ga1–N3 = 77.34(9), N1–Ga1–N3 = 153.85(10), Ga1–F1–Ga1a = 103.81(9).

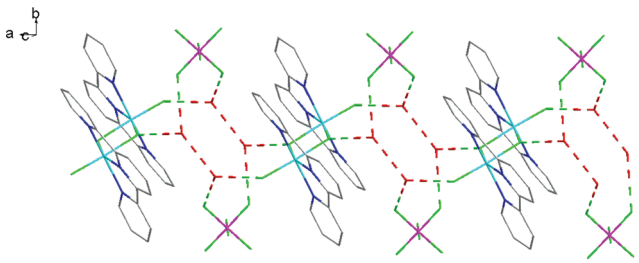

Fig. 8 View showing the H-bonding network (red) in $[\{Ga(terpy)F\}_2(\mu\text{-}F)_2][PF_6]_2\cdot 4H_2O$.

which means the neutral bipy ligand is *trans* to OH_2/F (Fig. 9 and 10).

For $[InF_3(bipy)(OH_2)]\cdot 2H_2O$,[13] In–$F_{transF}$ = 2.065(2), 2.070(2), In–F_{transN} = 2.002(3), In–N_{transF} = 2.260(4), In–N_{transO} = 2.243(4), In–O = 2.130(4) Å. Comparing the bond lengths in the three compounds reveals some interesting trends. The M–N distances are only slightly different (≤0.02 Å) between Al and Ga, whereas the M–F and M–O distances increase by between 0.06–0.1 Å; as noted with the terpy compounds above, the more electronegative donors have the greatest differences. The corresponding bond lengths all increase in the indium complex as expected, but here the differences with donor type are less clear, with all showing an increase of ~0.15–0.2 Å over the gallium analogue. In all of the complexes H-bonding to the lattice water and π-stacking of the aromatic rings is also evident (Fig. 11–13 and S2‡).

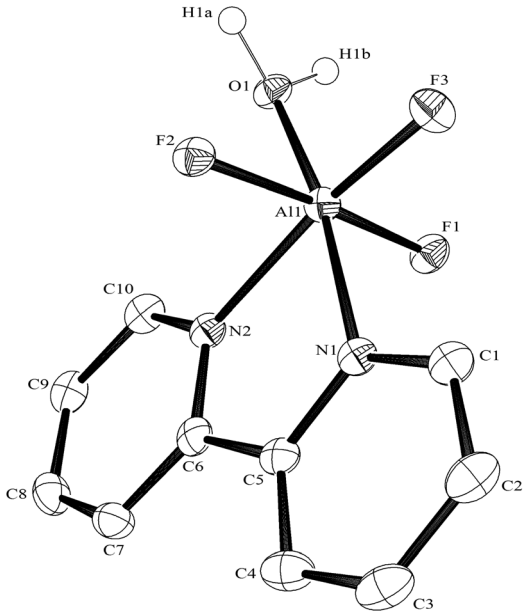

Fig. 9 The structure of the Al complex in $[AlF_3(bipy)(OH_2)]\cdot 2H_2O$ with ellipsoids drawn at the 50% probability level. Hydrogen atoms (except those on the coordinated water) are omitted for clarity. Selected bond lengths (Å) and angles (°): Al1–F1 = 1.786(2), Al1–F2 = 1.781(2), Al1–F3 = 1.743(2), Al1–O1 = 1.900(2), Al1–N1 = 2.050(3), Al1–N2 = 2.072(3), F2–Al1–F3 = 93.35(11), F1–Al1–F3 = 92.22(11), F3–Al1–O1 = 97.24(10), F2–Al1–O1 = 88.30(11), F1–Al1–O1 = 89.16(11), F3–Al1–N1 = 92.19(10), F2–Al1–N1 = 90.08(10), F1–Al1–N1 = 91.55(10), F2–Al1–N2 = 86.50(11), F1–Al1–N2 = 88.32(11), O1–Al1–N2 = 92.39(11), N1–Al1–N2 = 78.18(11).

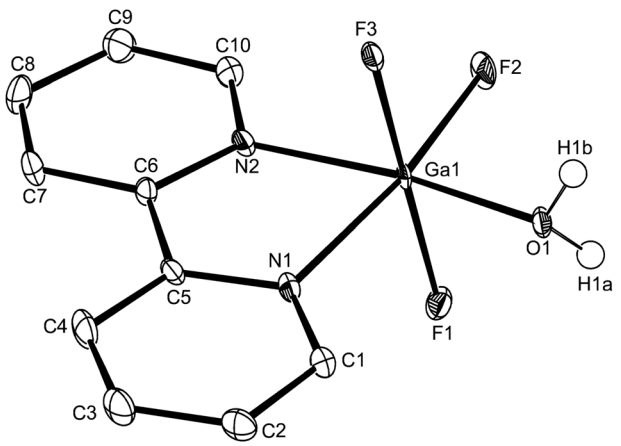

Fig. 10 The structure of Ga species in $[GaF_3(bipy)(OH_2)]\cdot 2H_2O$ with ellipsoids drawn at the 50% probability level. Hydrogen atoms (except those on the coordinated water) are omitted for clarity. Selected bond lengths (Å) and angles (°): Ga1–F1 = 1.8892(15), Ga1–F2 = 1.8442(17), Ga1–F3 = 1.8857(14), Ga1–O1 = 1.962(2), Ga1–N1 = 2.093(2), Ga1–N2 = 2.064(3), F2–Ga1–F3 = 92.41(7), F1–Ga1–F2 = 90.74(7), F1–Ga1–F3 = 175.68(7), F2–Ga1–O1 = 96.70(8), F3–Ga1–O1 = 87.76(7), F1–Ga1–O1 = 88.94(7), F2–Ga1–N2 = 92.28(9), F3–Ga1–N2 = 90.64(8), F1–Ga1–N2 = 92.19(8), F3–Ga1–N1 = 87.52(7), F1–Ga1–N1 = 89.86(7), O1–Ga1–N1 = 92.67(8), N2–Ga1–N1 = 78.35(9).

 This journal is © The Royal Society of Chemistry 2015

Open Access Article. Published on 20 April 2015. Downloaded on 11/26/2024 12:58:05 AM.
This article is licensed under a Creative Commons Attribution 3.0 Unported Licence.

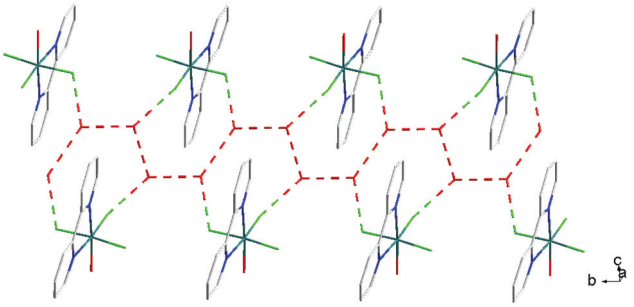

Fig. 11 View showing the H-bonding network (red) involving the F^- ligands and lattice H_2O present in the structure of $[AlF_3(bipy)(OH_2)]\cdot 2H_2O$.

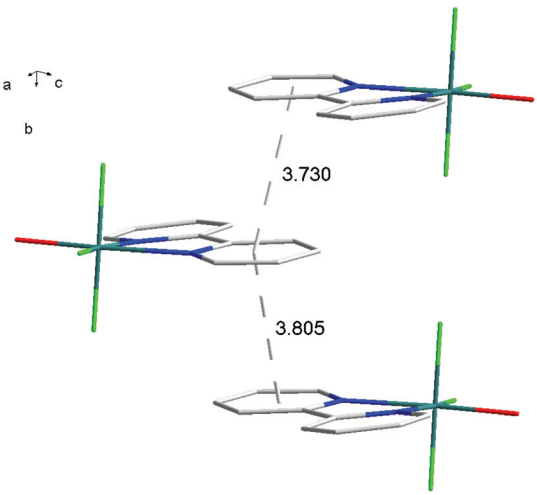

Fig. 12 View showing the π-stacking (lattice H_2O omitted for clarity) present in the structure of $[AlF_3(bipy)(OH_2)]\cdot 2H_2O$.

Overall, the structural data reinforce earlier conclusions that trends in the bond lengths in comparable Al and Ga complexes often differ from those predicted on the basis of simple Lewis acidity in the gas phase;[22,27–29] other factors, including the presence or absence of lattice solvent and hydrogen bonding also need to be considered.[13,19,21,22] The effects are less noticeable at indium, where corresponding bonds are typically ~0.2 Å longer than for Ga, reflecting the increased radius of the metal centre.

Using the same hydrothermal route with 1,10-phenanthroline in place of 2,2′-bipyridyl, gave $[MF_3(phen)(OH_2)]$, notably without lattice water (in contrast to the terpy and bipy complexes above). The structure of crystals of $[GaF_3(phen)(OH_2)]$ is shown in Fig. 14, and the $[InF_3(phen)(OH_2)]$ is isomorphous.[13] Corresponding bond lengths are again ~0.15–0.20 Å longer for the indium complex. The $[GaF_3(phen)(OH_2)]$ also shows π-stacking of the aromatic rings (Fig. S3‡) and intermolecular F···H hydrogen bonding, in this case involving the coordinated water molecules (Fig. 15).

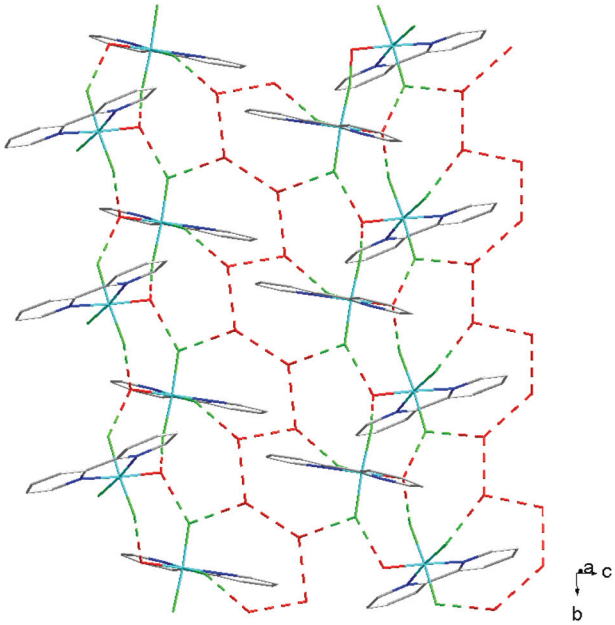

Fig. 13 View showing the H-bonding network (red) present in the structure of $[GaF_3(bipy)(OH_2)]\cdot 2H_2O$.

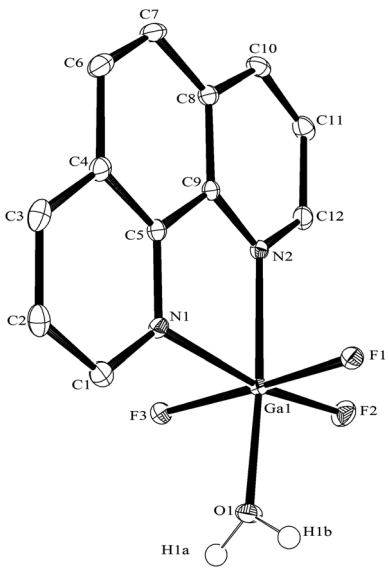

Fig. 14 The structure of $[GaF_3(phen)(OH_2)]$ with ellipsoids drawn at the 50% probability level. Hydrogen atoms (except those on the coordinated water) are omitted for clarity. Selected bond lengths (Å) and angles (°): Ga1–F1 = 1.8990(11), Ga1–F2 = 1.8242(12), Ga1–F3 = 1.8790(11), Ga1–N1 = 2.1250(16), Ga1–N2 = 2.0897(16), Ga1–O1 = 1.9594(14), F2–Ga1–F3 = 95.13(5), F1–Ga1–F2 = 93.69(5), F2–Ga1–O1 = 98.11(6), F3–Ga1–O1 = 89.79(5), F1–Ga1–O1 = 86.92(5), F2–Ga1–N2 = 92.02(6), F3–Ga1–N2 = 93.11(5), F1–Ga1–N2 = 88.65(5), F3–Ga1–N1 = 87.18(6), F1–Ga1–N1 = 84.47(6), O1–Ga1–N1 = 91.54(6), N2–Ga1–N1 = 78.20(6).

The IR spectra of the $[MF_3(phen)(OH_2)]$ complexes show quite weak features due to ν(OH) and δ(HOH), whereas in the hydrated $[MF_3(bipy)(OH_2)]\cdot 2H_2O$ the corresponding features

Open Access Article. Published on 20 April 2015. Downloaded on 11/26/2024 12:58:05 AM.
This article is licensed under a Creative Commons Attribution 3.0 Unported Licence.

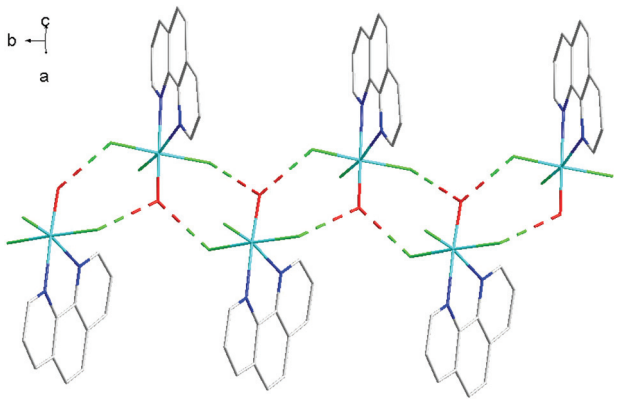

Fig. 15 View showing the H-bonding network (red) present in the structure of $[GaF_3(phen)(OH_2)]$.

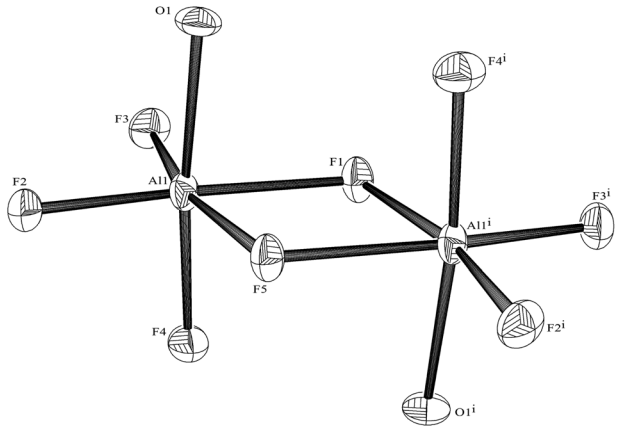

Fig. 16 The structure of the $[Al_2F_8(OH_2)_2]^{2-}$ anion with ellipsoids drawn at the 50% probability level and with (O–H) hydrogens omitted. Selected bond lengths (Å) and angles (°): Al1–F2 = 1.748(2), Al1– F3 = 1.749(2), Al1–F4 = 1.778(2), Al1–O1 = 1.895(2), Al1–F5 = 1.8968(19), Al1–F1 = 1.9048(19), F2–Al1–F3 = 99.65(11), F2–Al1–F4 = 93.28(10), F3–Al1–F4 = 93.83(10), F2–Al1–O1 = 90.62(10), F3–Al1–O1 = 90.65(10), F2–Al1–F5 = 92.34(10), F4–Al1–F5 = 88.95(8), O1–Al1–F5 = 85.68(8), F3–Al1–F1 = 91.94(10), F4–Al1–F1 = 88.61(8), O1–Al1–F1 = 86.52(8), F5–Al1–F1 = 75.93(10), Al1–F5–Al1^i = 104.38(13), Al1–F1–Al1^i = 103.77(13).

are much stronger and show several overlapping bands. The ν(MF) fall in energy as expected Al > Ga > In, but for the corresponding Al and Ga complexes (less clearly in the In complexes), those in $[MF_3(bipy)(OH_2)]\cdot 2H_2O$ occur at lower frequency than in $[MF_3(phen)(OH_2)]$, which is probably due to the extensive hydrogen bonding in the former.

The multinuclear NMR data show interesting trends as the metal is changed. The complexes were insoluble or very poorly soluble in chlorocarbons and CD_3CN, and therefore spectra were obtained from freshly prepared solutions in CD_3OD. The solutions decompose slowly forming F^- or HF_2^-, qualitatively the indium complexes seem less stable in solution than those of the lighter metals. At 183 K, all six complexes show two resonances with relative intensities 1 : 2 in the $^{19}F\{^1H\}$ NMR spectra, consistent with the solid state structures. On warming, the fluorine resonances of the indium complexes are lost, and those of the gallium complexes and of $[AlF_3(bipy)(OH_2)]$ broaden and then coalesce; only the $^{19}F\{^1H\}$ NMR spectrum of $[AlF_3(phen)(OH_2)]$ shows two fluorine resonances at room temperature. The ^1H NMR spectra of the aluminium complexes show inequivalent pyridyl rings, as expected from the static structures, but those of the gallium and indium show broad resonances even at low temperatures. The temperature dependence of the spectra is consistent with reversible ligand dissociation, possibly of the water, to give a fluxional five-coordinate intermediate, the dissociation increasing with decreased Lewis acid strength Al > Ga > In.

Reactions of $MF_3\cdot 3H_2O$ with PMDTA

PMDTA, $Me_2N(CH_2)_2NMe(CH_2)_2NMe_2$, is a flexible, aliphatic acyclic triamine analogue of Me_3-tacn and terpy, and its reactions with the hydrated Group 13 fluorides were explored to provide a third series of complexes for comparison. In contrast to the reactions with the other two N_3-donor ligands, the hydrothermal route using PMDTA resulted in cleavage of the triamine and the formation of the 1,1,4-trimethylpiperazinium cation, $[\subset Me_2N(CH_2)_2NMe(CH_2)_2]^+$. After removing all volatiles from the reaction mixtures and washing the residue with MeCN, the ^1H and $^{13}C\{^1H\}$ NMR spectra show the cyclic cation to be the only organic species in the bulk products. For the aluminium reaction, crystals were obtained, showing the solid contained $[\subset Me_2N(CH_2)_2NMe(CH_2)_2]_2[Al_2F_8(OH_2)_2]\cdot 2H_2O$. The anion (Fig. 16) has been obtained previously as the $[NMe_4]^+$ salt,[32] and breaks up in solution to form $[AlF_4]^-$, which was identified by a combination of ^{27}Al (δ = 48.7 (s)) and $^{19}F\{^1H\}$ NMR data (δ = –194.6, 6 lines, $^1J_{AlF}$ = 38 Hz).[32]

In the cases of the gallium and indium reactions, a few crystals of the same cation were obtained as the chloride salt, from traces of chloride in the reaction. The structure of $[\subset Me_2N(CH_2)_2NMe(CH_2)_2]Cl$ has been reported previously[31] and the crystals obtained in this study were identical, and hence are not discussed further (see ESI‡). The data on the bulk product from the gallium reaction fitted the constitution $[\subset Me_2N(CH_2)_2NMe(CH_2)_2]_2\ [Ga_2F_8(OH_2)_2]\cdot 2H_2O$, analogous to the aluminium complex, although in the absence of X-ray structural data, the anion present cannot be confirmed. The relative instability of the fluoro-metallate anions in solution and the sensitivity of the ^{19}F chemical shifts to solvent,[30,32] make identification of the anions uncertain without structural data. The reactions of the $MF_3\cdot 3H_2O$ with PMDTA were also attempted in refluxing methanol solution, since it was reasoned that the milder conditions (compared to the hydrothermal preparations) might have prevented cleavage of the PMDTA. No reaction occurred in the case of indium fluoride, whilst with $AlF_3\cdot 3H_2O$, ^1H and $^{19}F\{^1H\}$ NMR spectra of the crude product showed protonated PMDTA and $[AlF_4]^-$ as the only significant species. The contrast between the instability of PMDTA and the robust Me_3-tacn which has similar groups in these Group 13 fluoride reactions may be due to the ring structure of the latter preventing close approach of an amine

 This journal is © The Royal Society of Chemistry 2015

Open Access Article. Published on 20 April 2015. Downloaded on 11/26/2024 12:58:05 AM.
This article is licensed under a Creative Commons Attribution 3.0 Unported Licence.

function polarised by coordination to the metal, to the next CH_2NMe unit, which is presumably the first stage in C–N bond fission and formation of the small ring.

Conclusions

Hydrothermal synthesis using $MF_3{\cdot}3H_2O$ as the metal source has been shown to be a convenient method to form a range of complexes of the otherwise rather intractable Group 13 trifluorides with nitrogen heterocycles in high yield. X-Ray crystallographic studies show all of the new complexes contain a *mer* arrangement of fluorides, contrasting with the *fac* geometry present in the triaza-macrocyclic complexes[15] reported previously. Extensive H-bonding and π-stacking networks are present in the complexes of all three imines with the three metal ions, although the details differ. These studies significantly extend the known coordination chemistry of the Group 13 trifluorides. The relatively high stability of the trifluoride complexes contrasts with the moisture sensitivity of complexes of the Group 13 elements with heavier halides. However, this work has also shown that unlike $[GaF_3(BzMe_2\text{-tacn})]{\cdot}4H_2O$, which is stable towards alkali metal or ammonium salts in aqueous MeCN, forming heterometallic (or mixed gallium-ammonium) complexes, competitive ions such as $[NH_4]^+$ and $[PF_6]^-$, $[GaF_3(terpy)]{\cdot}3H_2O$ reacts, with loss of a fluoride ligand, to form the dinuclear product, $[\{Ga(terpy)F\}_2(\mu\text{-}F)_2][PF_6]_2{\cdot}4H_2O$.

Future work will aim to establish whether the hydrothermal approach is also suitable for oxygen donor ligands and whether soft donor ligands such as thioethers or phosphines can form complexes with the Group 13 fluorides.

Acknowledgements

We thank EPSRC and GE Healthcare for support (EP/I501673/1, EP/L505651/1 and EP/1033394/1).

References

1 (*a*) S. L. Benjamin, W. Levason and G. Reid, *Chem. Soc. Rev.*, 2013, **42**, 1460; (*b*) *Chemistry of aluminium, gallium, indium and thallium*, ed. A. J. Downs, Blackie, London, 1st edn, 1993.
2 (*a*) E. Kemnitz, U. Gross, St. Ruediger, G. Scholz, D. Heideman, S. I. Troyanov, I. V. Morosov and M.-H. Lemee-Cailleau, *Solid State Sci.*, 2006, **8**, 1443; (*b*) P. Bukovec and V. Kaucic, *Inorg. Nucl. Chem. Lett.*, 1978, **14**, 79.
3 S. Petricek, A. Demsar, P. Bukovec, L. Golic and J. V. Brencic, *Acta Chim. Slov.*, 1997, **44**, 317.
4 F. N. Penkert, T. Weyhermuller and K. Wieghardt, *Chem. Commun.*, 1998, 557.
5 D. R. Ketchum, G. L. Schimek, W. T. Pennington and J. W. Kolis, *Inorg. Chim. Acta*, 1999, **294**, 200.
6 (*a*) M. Roos and G. Meyer, *Z. Anorg. Allg. Chem.*, 1999, **625**, 1129. M. Roos and G. Meyer, *Z. Anorg. Allg. Chem.*, 1999, **625**, 1843.
7 S. A. Polyshchuk, S. P. Kozerenko and Y. V. Gagarinsky, *J. Less-Common Met.*, 1972, **27**, 45.
8 S. P. Kozerenko, S. A. Polyshchuk and N. I. Sigula, *Russ. J. Inorg. Chem.*, 1972, **17**, 954.
9 M. Roos, J. Wittrock, G. Meyer, S. Fritz and J. Straehle, *Z. Anorg. Allg. Chem.*, 2000, **626**, 1179.
10 S. P. Petrosyants and E. R. Buslaeva, *Russ. J. Inorg. Chem.*, 1989, **34**, 932.
11 S. A. Polyshchuk and G. F. Krysenko, *Koord. Khim.*, 1977, **3**, 816.
12 M. A. Malyarik, S. P. Petrosyants, A. B. Ilyukhin and Yu. A. Buslaev, *Russ. J. Inorg. Chem.*, 1991, **36**, 2816.
13 (*a*) A. B. Ilyukhin and M. A. Malyarik, *Koord. Khim.*, 1999, **44**, 1511; (*b*) A. B. Ilyukhin and M. A. Malyarik, *Krystallographiya*, 1994, **39**, 439.
14 S. P. Petrosyants and A. B. Ilyukhin, *Russ. J. Inorg. Chem.*, 2010, **55**, 30.
15 R. Bhalla, C. Darby, W. Levason, S. K. Luthra, G. McRobbie, G. Reid, G. W. Sanderson and W. Zhang, *Chem. Sci.*, 2014, **5**, 381.
16 (*a*) A. Dimitrov, D. Heidemann, K. I. Khallow and E. Kemnitz, *Inorg. Chem.*, 2012, **51**, 11612; (*b*) A. Dimitrov, D. Heidemann and E. Kemnitz, *Inorg. Chem.*, 2006, **45**, 10807.
17 (*a*) P. Laverman, W. McBride, R. Sharkey, A. Eek, L. Joosten, W. Oyen, D. Goldenberg and O. Boerman, *J. Nucl. Med.*, 2010, **51**, 454; (*b*) W. McBride, C. D'Souza, R. Sharkey, H. Karacay, E. Rossi, C. Chang and D. Goldenberg, *Bioconjugate Chem.*, 2010, **21**, 1331; (*c*) W. McBride, R. Sharkey, H. Karacay, C. D'Souza, E. Rosso, P. Laverman, C. Chang, O. Boerman and D. Goldenberg, *J. Nucl. Med. Chem.*, 2009, **50**, 991; (*d*) W. McBride, C. D'Souza, H. Karacay, R. Sharkey and D. Goldenberg, *Bioconjugate Chem.*, 2012, **23**, 538; (*e*) D. Shetty, S. Y. Choi, J. M. Jeong, J. Y. Lee, L. Hoigebazar, Y.-S. Lee, D. S. Lee, J. K. Chung, M. C. Lee and Y. K. Chung, *Chem. Commun.*, 2011, **47**, 9732; (*f*) R. Bhalla, W. Levason, S. K. Luthra, G. McRobbie, G. Sanderson and G. Reid, *Chem. – Eur. J.*, 2015, **21**, 4688.
18 G. M. Sheldrick, *Acta Crystallogr., Sect. A: Fundam. Crystallogr.*, 2008, **64**, 112.
19 I. V. Kazakov, M. Bodensteiner and A. Y. Timoshkin, *Acta Crystallogr., Sect. C: Cryst. Struct. Commun.*, 2014, **70**, 312.
20 (*a*) M. J. Taylor and P. J. Brothers, in *The chemistry of aluminium, gallium, indium and thallium*, ed. and A. J. Downs, Blackie, London, 1993, p. 111; (*b*) B. Cordero, V. Gomez, A. E. Platero-Prats, M. Reves, J. Echeverria, E. Cremades, F. Barragan and S. Alvarez, *Dalton Trans.*, 2008, 2832.
21 (*a*) J. Burt, W. Levason, M. E. Light and G. Reid, *Dalton Trans.*, 2014, **43**, 14600; (*b*) K. George, M. Jura, W. Levason, M. E. Light and G. Reid, *Dalton Trans.*, 2014, **43**, 3637.
22 A. Y. Timoshkin, M. Bodensteiner, T. N. Sevastianova, A. S. Lisovenko, E. I. Davydova, M. Scheer, C. Grassi and A. V. Butlak, *Inorg. Chem.*, 2012, **51**, 11602.
23 ^{27}Al [I = 5/2, 100% abundance, Ξ = 26.08 MHz, $Q = 0.149 \times 10^{-28}$ m^2, R_C = 1170], ^{69}Ga [I = 3/2, 60.4% abundance, Ξ =

Open Access Article. Published on 20 April 2015. Downloaded on 11/26/2024 12:58:05 AM.
This article is licensed under a Creative Commons Attribution 3.0 Unported Licence.

24.07 MHz, Q = 0.178 × 10^{-28} m^2, R_C = 237] ^{71}Ga [I = 3/2, 39.6% abundance, Ξ = 30.58 MHz, Q = 0.112 × 10^{-28} m^2, R_C = 322] ^{115}In [I = 9/2, 95.7% abundance, Ξ = 22.04 MHz, Q = 1.16 × 10^{-28} m^2, R_C = 1920].

24 J. Mason, *Multinuclear NMR*, Plenum, New York, 1987.

25 R. Bhalla, W. Levason, S. J. Luthra, G. McRobbie, G. Reid, G. Sanderson and W. Zhang, *Chem. Commun.*, 2014, **50**, 12673.

26 K. S. Pedersen, G. Lorusso, J. J. Morales, T. Weyhermuller, S. Piligkos, S. K. Singh, D. Larsen, M. Schau-Magnussen, G. Rajaraman, M. Evanelisti and J. Bendix, *Angew. Chem., Int. Ed.*, 2014, **53**, 2394.

27 F. Bessac and G. Frenking, *Inorg. Chem.*, 2006, **45**, 6956.

28 J. Burt, W. Levason and G. Reid, *Coord. Chem. Rev.*, 2014, **260**, 65, and refs therein.

29 A. V. Timoshkin, A. V. Suvorov, H. F. Bettinger and H. F. Schaefer III, *J. Am. Chem. Soc.*, 1999, **121**, 5687.

30 (*a*) N. Herron, D. L. Thorn, R. L. Harlow and F. Davidson, *J. Am. Chem. Soc.*, 1993, **115**, 3028; (*b*) N. Herron, R. L. Harlow and D. L. Thorn, *Inorg. Chem.*, 1993, **32**, 2985.

31 W. Massa and K. Dehnicke, *Z. Anorg. Allg. Chem.*, 2009, **635**, 287.

32 S. P. Petrosyants and A. B. Ilyukhin, *Russ. J. Inorg. Chem.*, 2011, **56**, 1250.

 This journal is © The Royal Society of Chemistry 2015